Supporting Information

Gaussian Accelerated Molecular Dynamics Uncovers Binding Mechanism Differences Between Small-Molecule Inhibitors and Grp94/Hsp90α: Elucidating Small Molecules' Selectivity for Grp94

Henglei Zhang,[a] Enhong Liu,[a] Jianzhong Chen*[b] and Xinguo Liu*[a]

[a] School of Physics and Optoelectronics, Shandong Normal University, Jinan, China 250358.

E-mail: liuxinguo@sdnu.edu.cn

[b] School of Science, Shandong Jiaotong University, Jinan, China 250357.

E-mail: jzchen@sdjtu.edu.cn, chenjianzhong1970@163.com

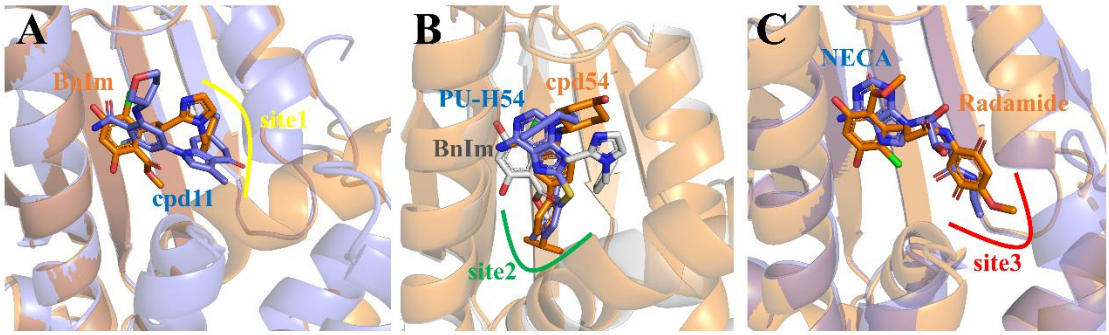

Fig. S1 Small-molecule inhibitors occupying the selective site of Grp94: (A) conformational superimposition of BnIm and cpd11 bound to site 1, (B) conformational superimposition of BnIm, PU-H54 and cpd54 bound to site 2, and (C) conformational superimposition of NECA and Radamide bound to site 3.

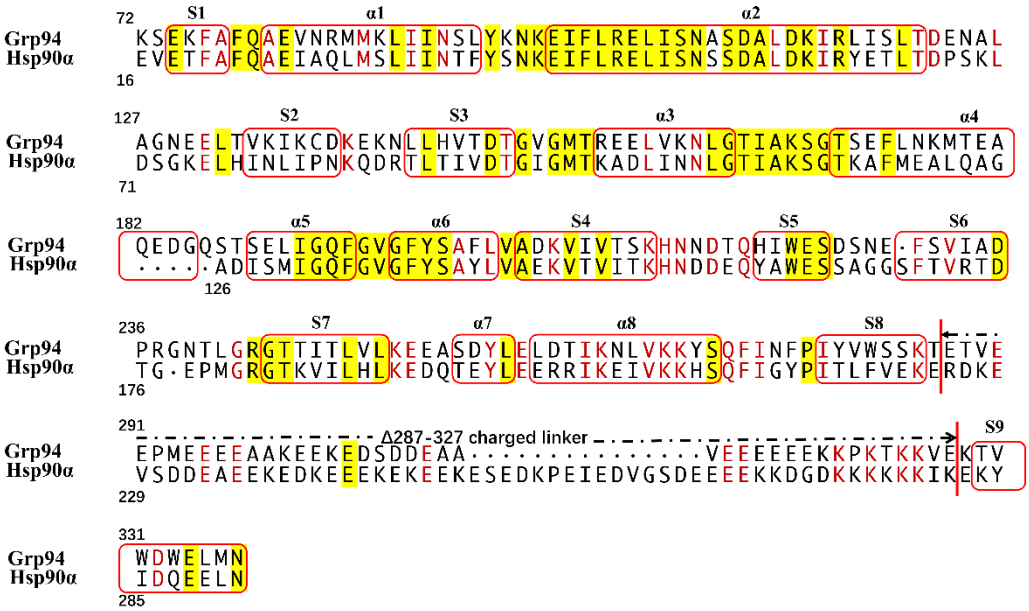

Fig. S2 The residue sequence arrangement of the N-terminal domains of Grp94 and Hsp90α (yellow background indicates that this residue is fully conserved among the four homologs; red font denotes that this residue is partially conserved between Grp94 and Hsp90α; and the red boxed regions represent the secondary structures within the protein).

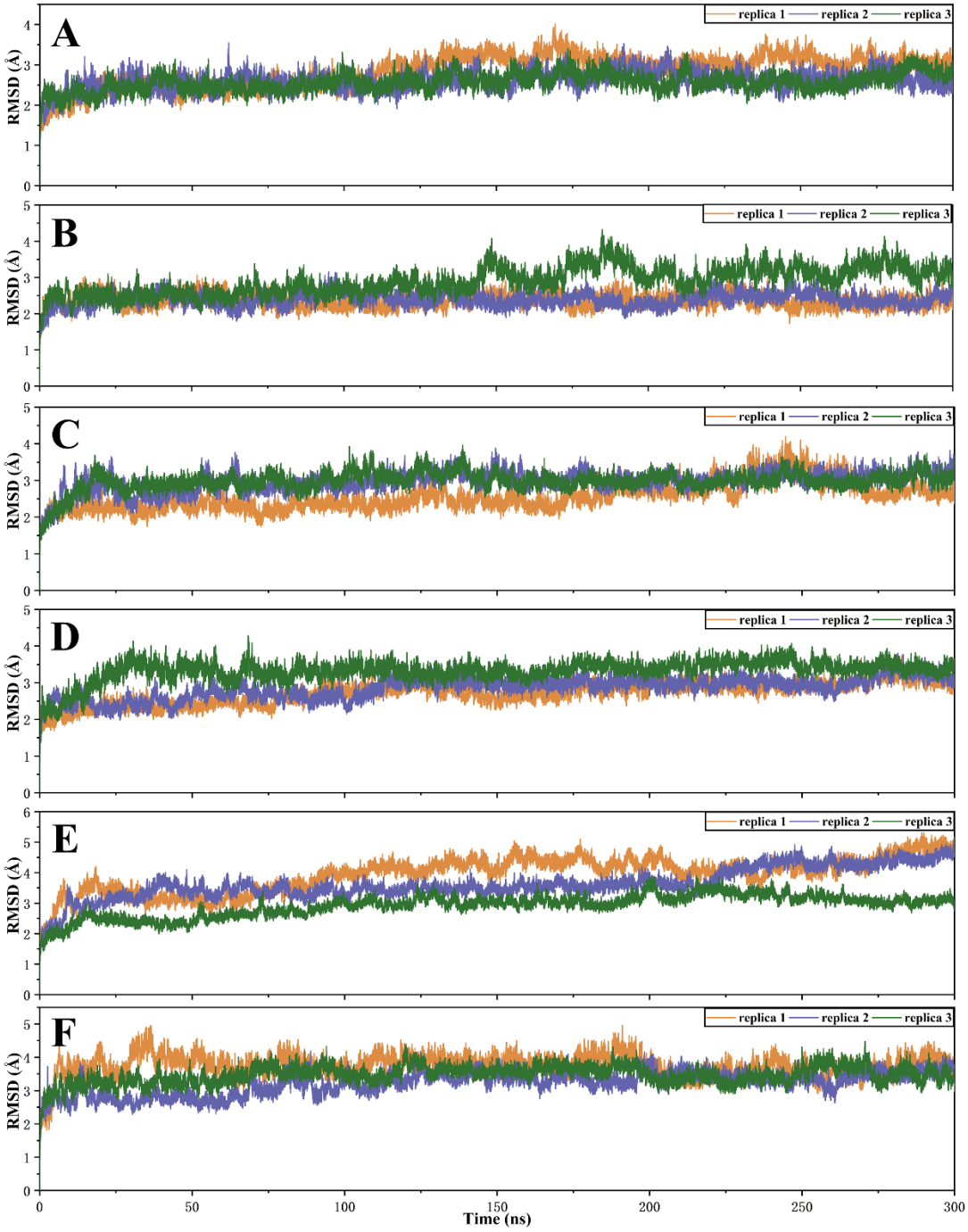

Fig. S3 The RMSDs corresponding to all replicas of the systems containing Grp94: (A) *apo*-N, (B) Grp94-NPCA, (C) *apo*-H, (D) Grp94-H36, (E) *apo*-B, and (F) Grp94-BnIm1.

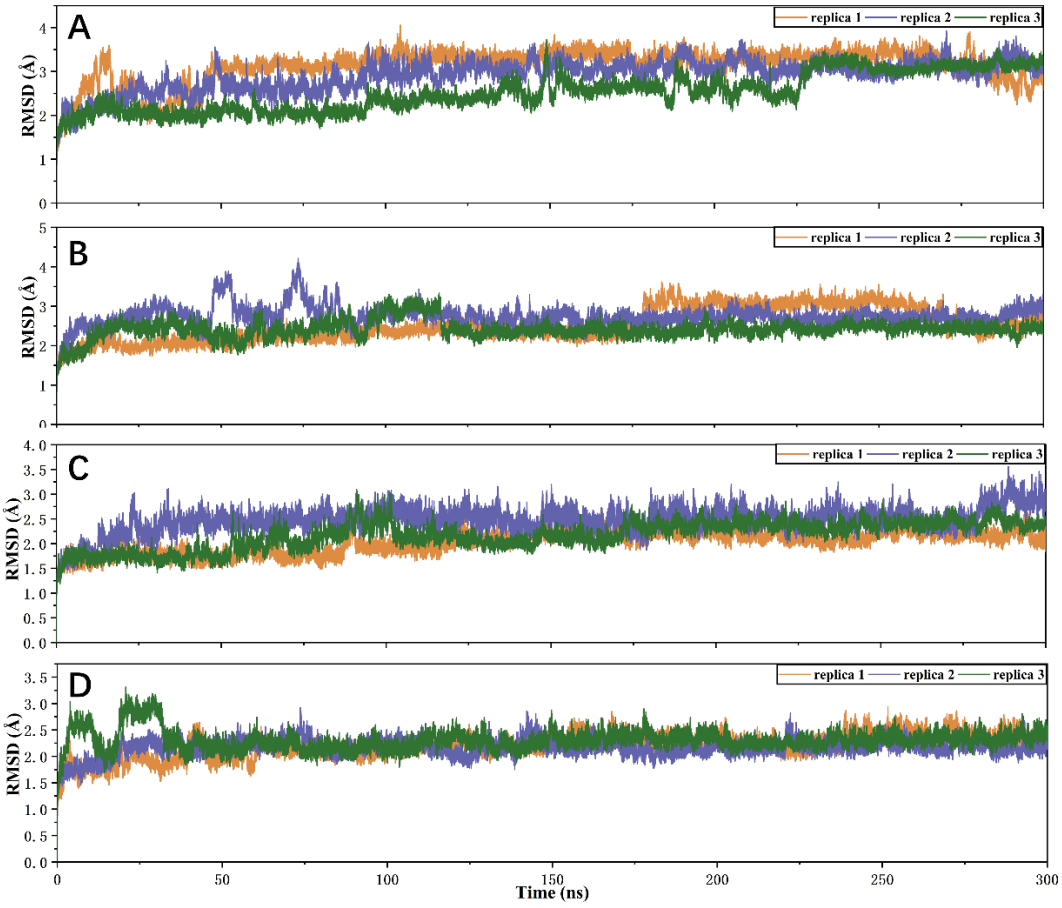

Fig. S4 The RMSDs corresponding to all replicas of the systems containing Hsp90α: (A) *apo*-Hsp90α, (B) Hsp90α-NPCA, (C) Hsp90α-H36, and (D) Hsp90α-BnIm1.

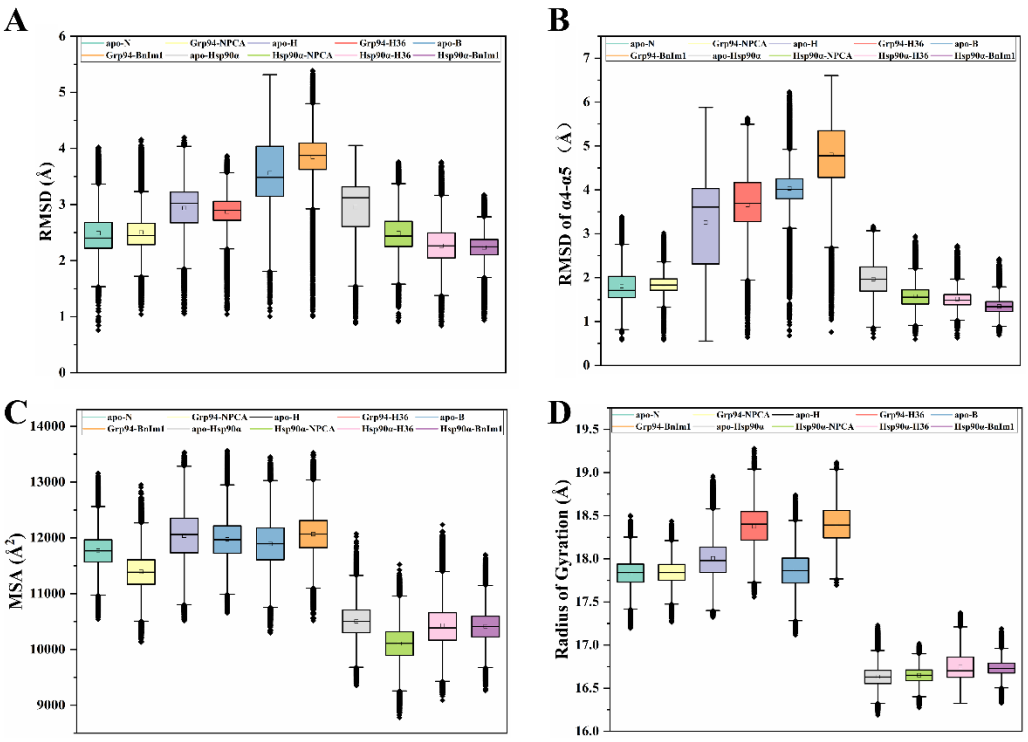

Fig. S5 RMSD, MSA, and RG reveal conformational dynamic changes of Grp94/Hsp90α induced by ligand binding: (A) the RMSDs of the backbone atoms in each system, (B) the RMSDs of the α4-α5 in each system, (C) the MSA of all systems, and (D) the Radius of Gyration of all systems.

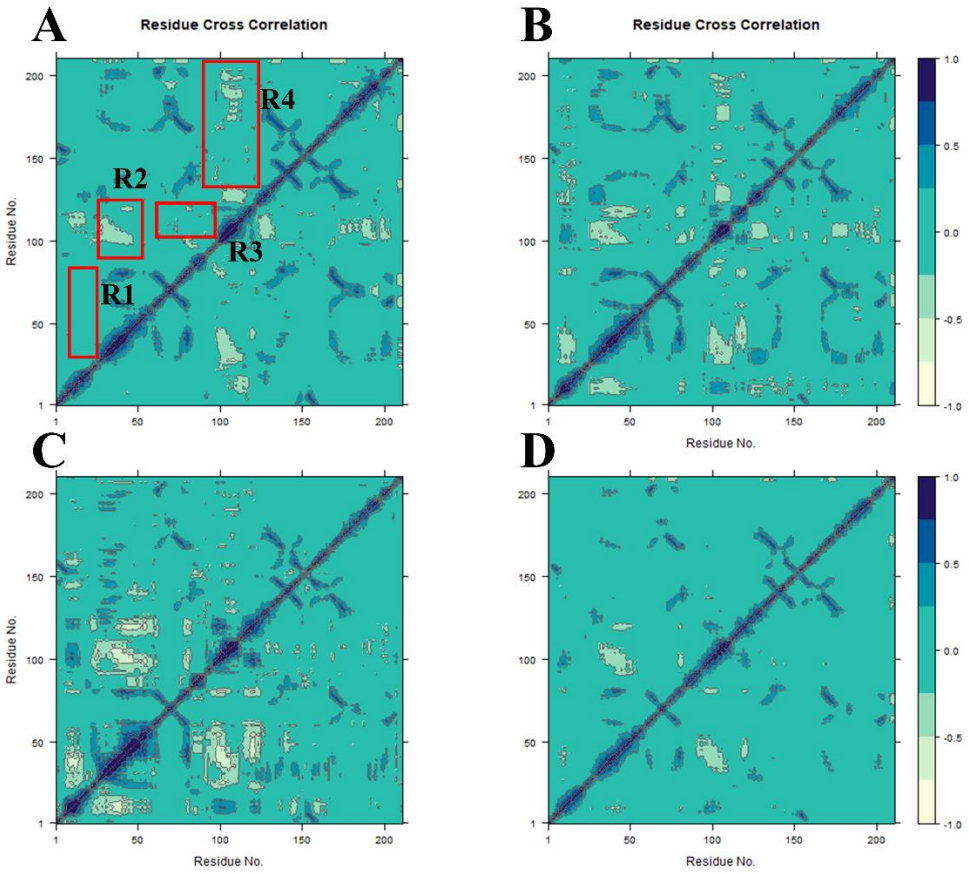

Fig. S6 DCCMs calculated by using the coordinates of the C_α atoms in GaMD trajectories: (A) *apo*- Hsp90α, (B) Hsp90α-NPCA, (C) Hsp90α-H36, and (D) Hsp90α-BnIm1.

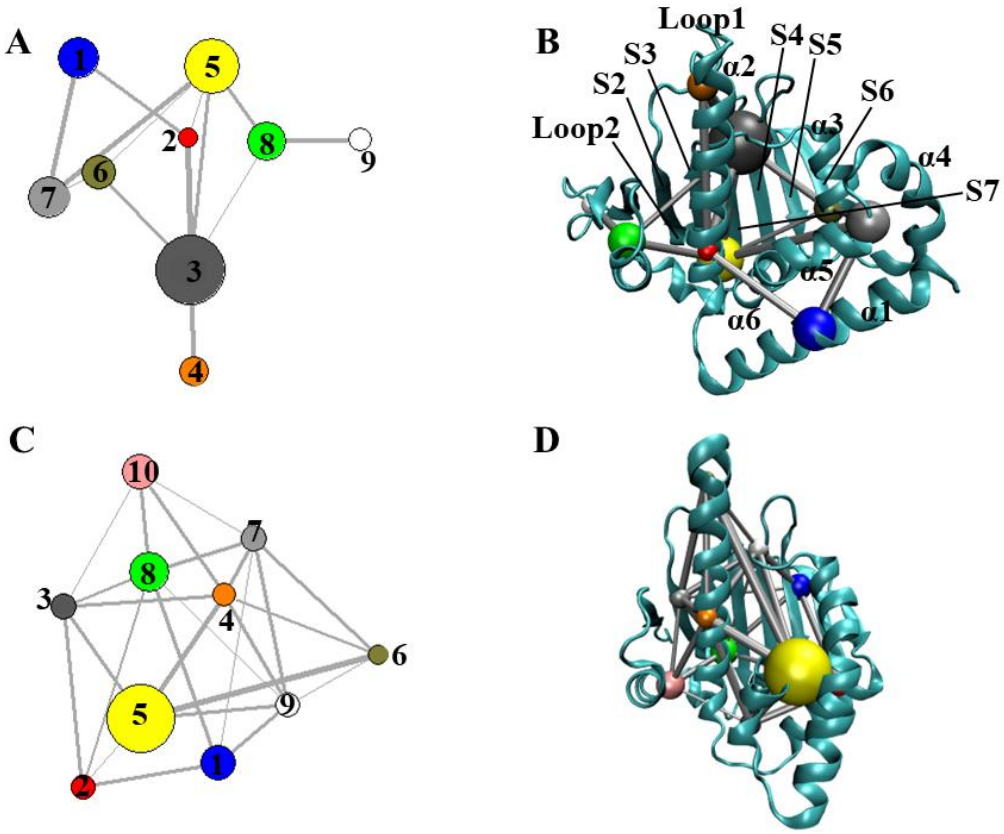

Fig. S7 H36 binding induces changes in the communication networks of Grp94 and Hsp90α: (A) cluster network of Grp94-H36, (B) projections of network in Grp94, (C) cluster network of Hsp90α-H36, and (D) projections of network in Hsp90α. In this figure, balls are used to represent nodes and sticks are adopted to indicate edges describing communications between different nodes.

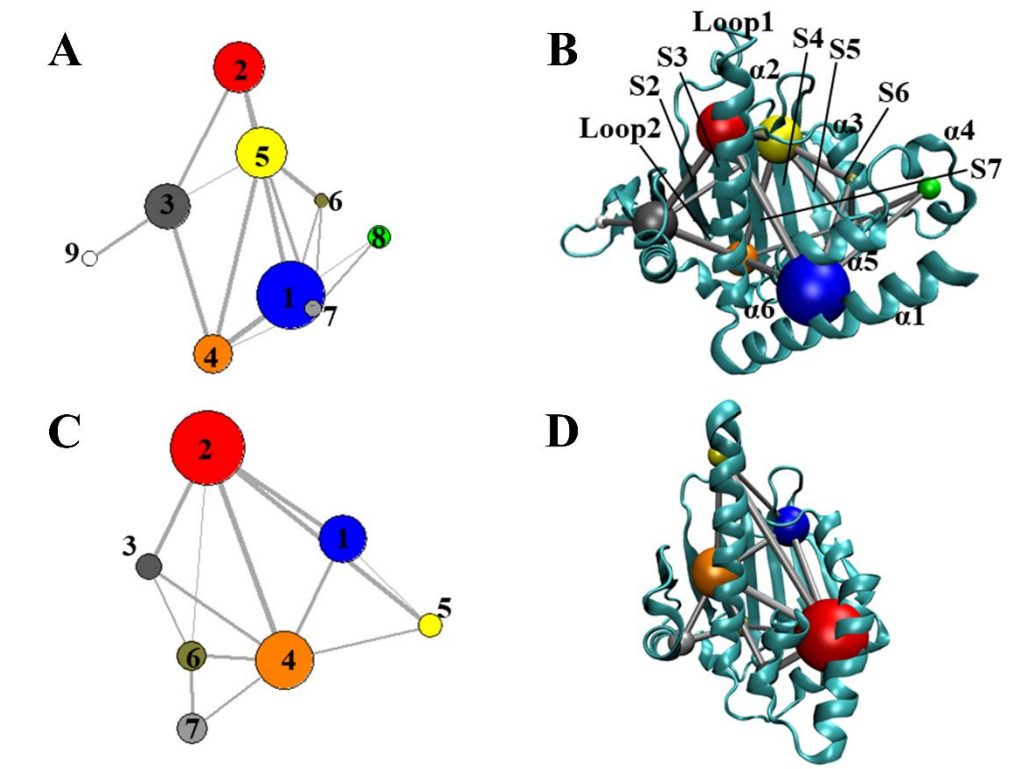

Fig. S8 BnIm1 binding induces changes in the communication networks of Grp94 and Hsp90α: (A) cluster network of Grp94-BnIm1, (B) projections of network in Grp94, (C) cluster network of Hsp90α-BnIm1, and (D) projections of network in Hsp90α. In this figure, balls are used to represent nodes and sticks are adopted to indicate edges describing communications between different nodes.

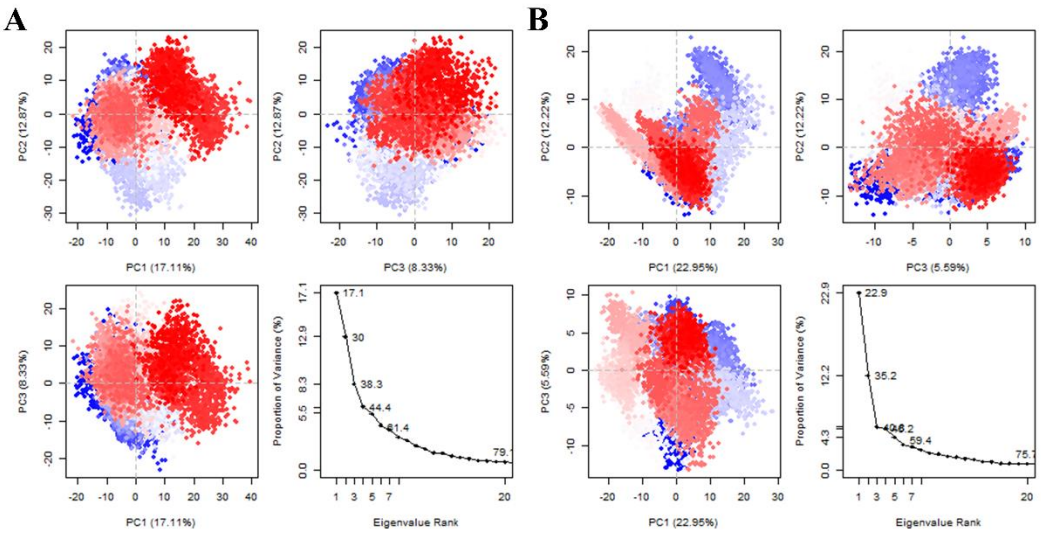

Fig. S9 Conformational cluster and the proportion of total fluctuation accounted for by the first 20 principal components: (A) Grp94-NPCA and (B) Hsp90α-NPCA.

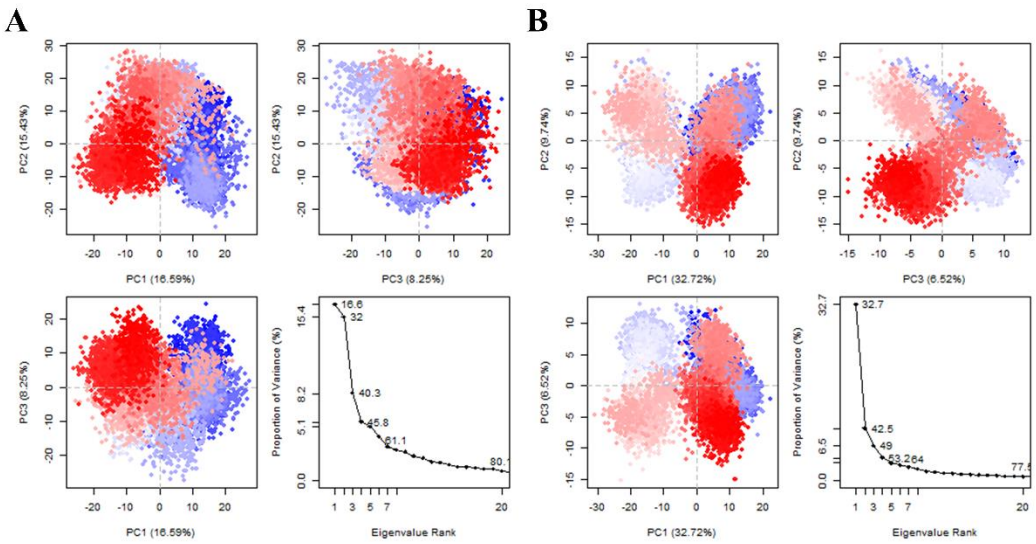

Fig. S10 Conformational cluster and the proportion of total fluctuation accounted for by the first 20 principal components: (A) Grp94-H36 and (B) Hsp90α-H36.

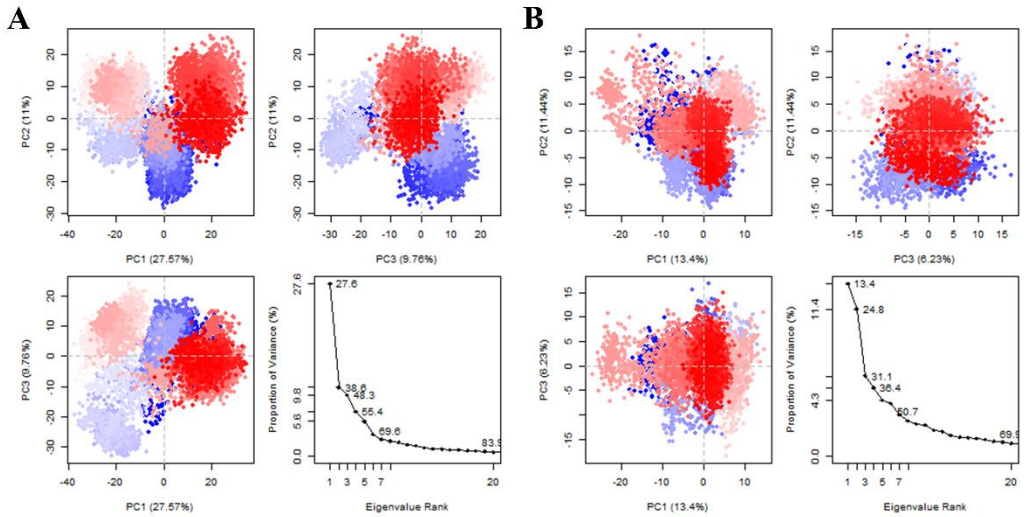

Fig. S11 Conformational cluster and the proportion of total fluctuation accounted for by the first 20 principal components: (A) Grp94-BnIm1 and (B) Hsp90α-BnIm1.

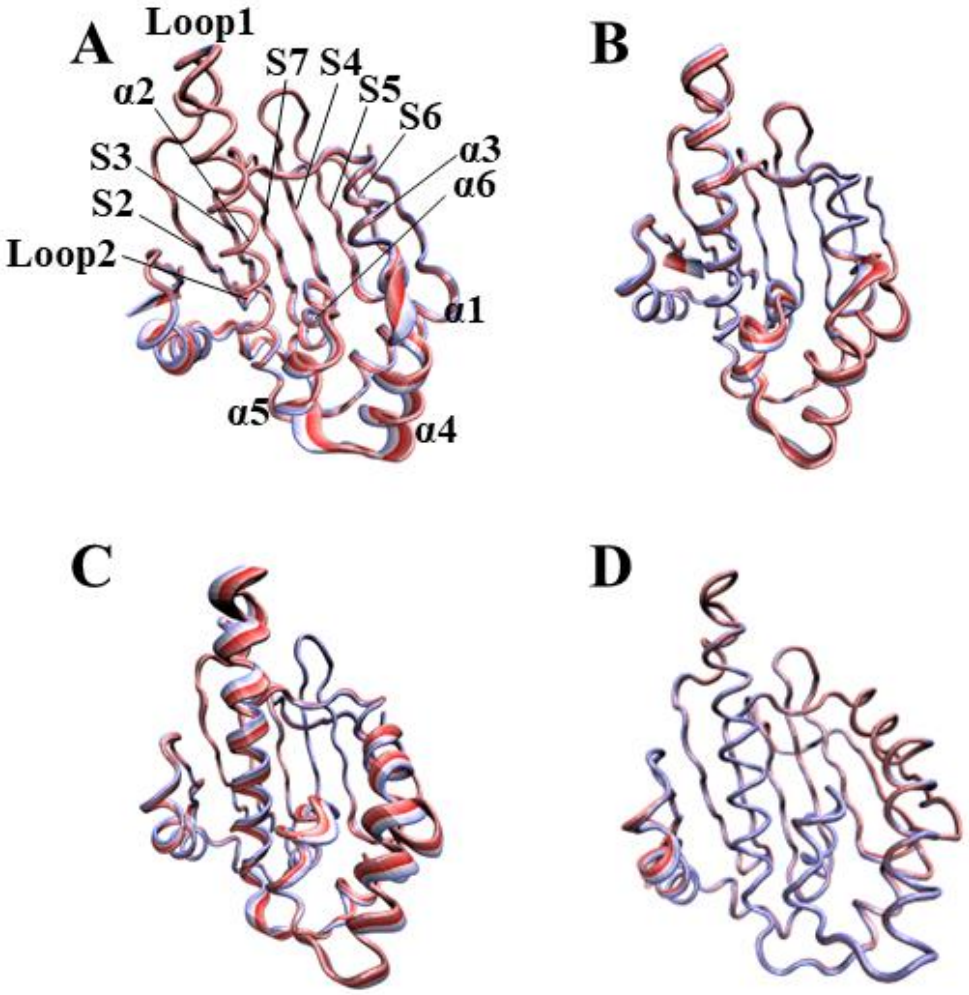

Fig. S12 Conformational dynamics of significant structure domains revealed by PCA: (A) *apo*- Hsp90α, (B) Hsp90α-NPCA, (C) Hsp90α-H36, and (D) Hsp90α-BnIm1.

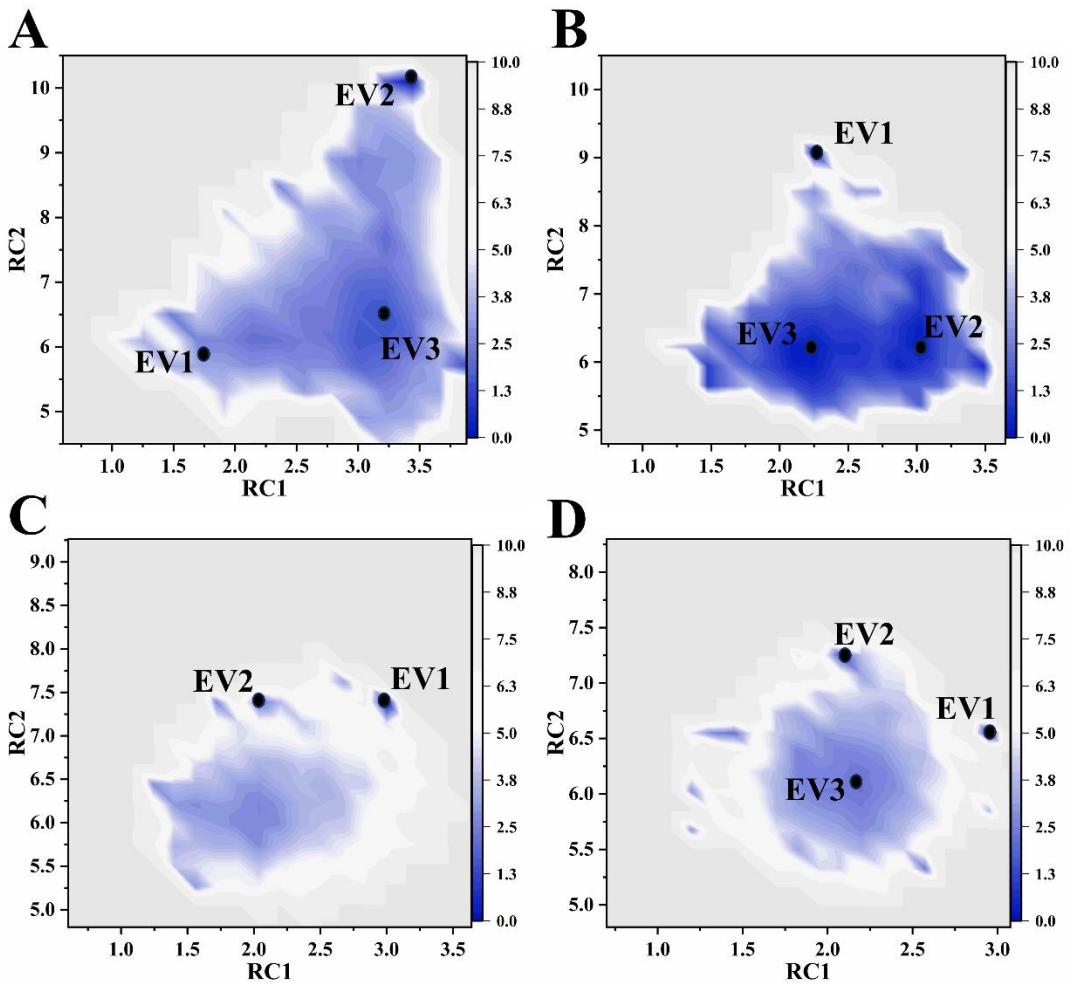

Fig. S13 The FEL diagrams of the system containing Hsp90α: (A) *apo*- Hsp90α, (B) Hsp90α-NPCA, (C) Hsp90α-H36, and (D) Hsp90α-BnIm1.

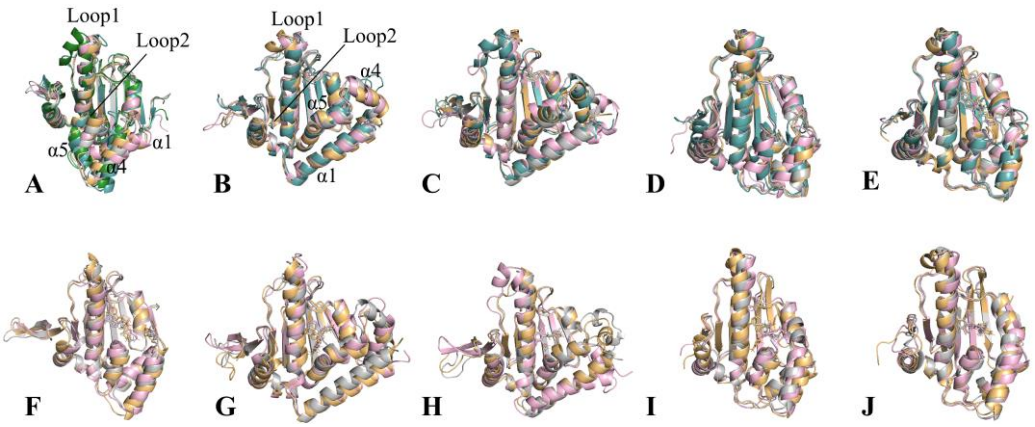

Fig. S14 The structural superposition for initial structure and conformational minima of each EVs: (A) *apo*-N, (B) *apo*-H, (C) *apo*-B, (D) *apo*-Hsp90α, (E) Hsp90α-NPCA, (F) Grp94-NPCA, (G) Grp94-H36, (H) Grp94-BnIm1, (I) Hsp90α-H36, and (J) Hsp90α-BnIm1.

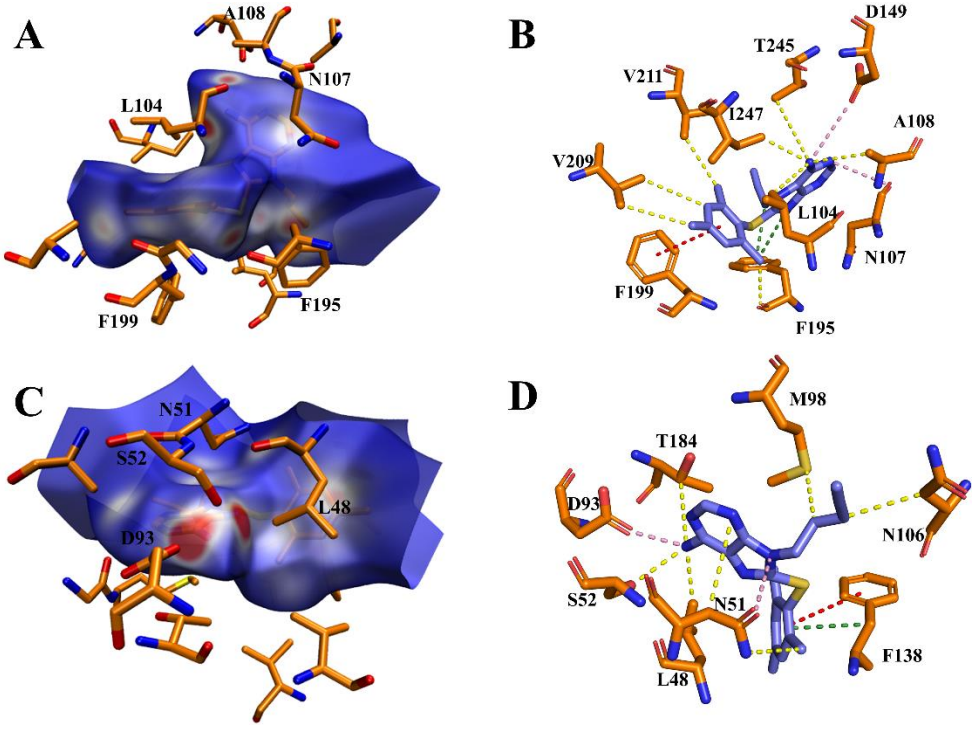

Fig. S15 Binding pocket and key ligand-residue interactions: (A) Hirshfeld surface results of Grp94-H36, (B) details of interactions with high intensity on the Hirshfeld surface in Grp94-H36, (C) Hirshfeld surface results of Hsp90α-H36, and (D) details of interactions with high intensity on the Hirshfeld surface in Hsp90α-H36.

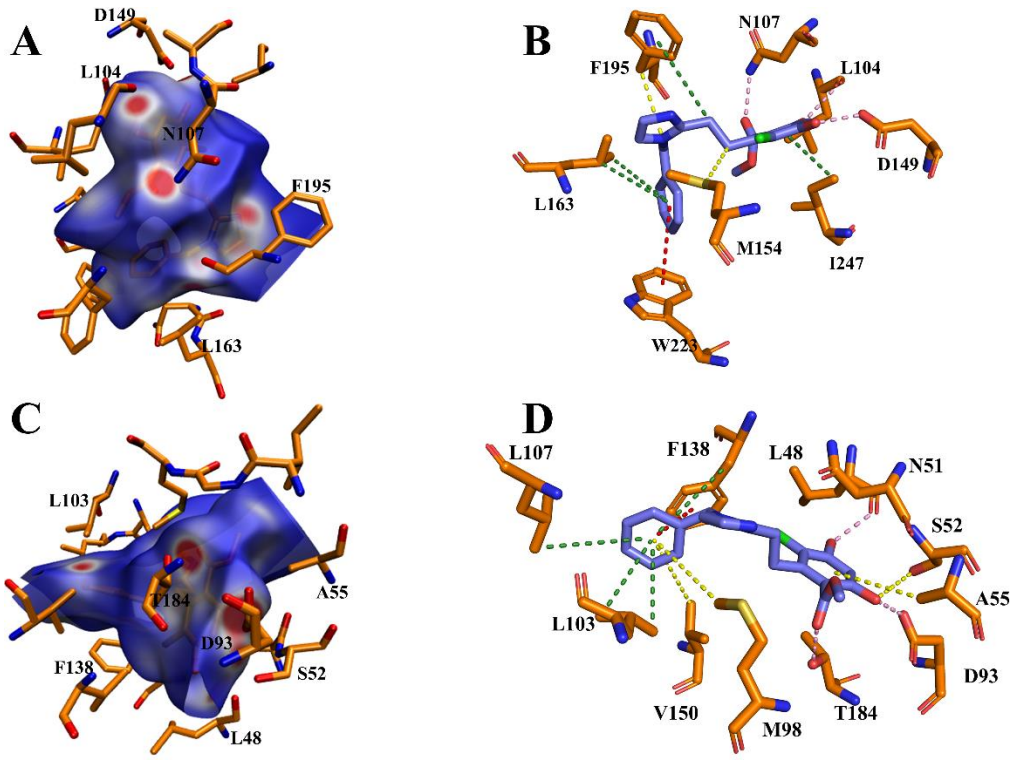

Fig. S16 Binding pocket and key ligand-residue interactions: (A) Hirshfeld surface results of Grp94-BnIm1, (B) details of interactions with high intensity on the Hirshfeld surface in Grp94-BnIm1, (C) Hirshfeld surface results of Hsp90α-BnIm1, and (D) details of interactions with high intensity on the Hirshfeld surface in Hsp90α-BnIm1.

Table S1 Hydrogen bonding interactions of inhibitors with the Grp94/Hsp90α.

Complexes	Hydrogen bonds[a]	Distancea(Å)	Anglea(deg)	Occupancy[b](%)
Grp94-NPCA	N107-ND2-HD21···LIG-O5‘	2.91	160.07	95.8
	G153-N-H···LIG-N1	3.16	153.95	87.8
	G153-N-H···LIG-N6	3.14	136.78	60.6
	V152-N-H···LIG-N1	3.00	140.27	56.9
	T245-OG1-HG1···LIG-N7	2.93	150.85	56.5
	LIG-N6-H17···D149-OD2	2.80	147.53	82.1
	LIG-N6-H16···T245-OG1	2.99	159.03	62.0
Grp94-H36	N107-ND2-HD21···LIG-NO4	2.97	161.38	99.1
	LIG-NO1-H21···D149-OD2	2.98	157.72	98.6
Grp94-BnIm1	N107-ND2-HD22···LIG-OAB	2.93	156.09	75.0
	LIG-OAC-H18···D149-OD1	2.56	163.45	100
	LIG-OAD-H19···L104-O	2.91	137.86	83.9
Hsp90α-NPCA	LIG-N6-H61···D93-OD2	2.88	154.41	98.2
	LIG-N5-H5···N106-O	2.97	158.68	69.3
Hsp90α-H36	N51-ND2-HD21···LIG-NO4	2.94	159.39	99.7
	LIG-NO1-H20···D93-OD2	2.94	148.69	95.9
Hsp90α-BnIm1	T184-OG1-HG1···LIG-OAB	2.78	163.52	97.9
	LIG-OAD-HAD···D93-OD2	2.57	168.32	100
	LIG-OAC-HAT···L48-O	2.98	137.44	71.1

[a] Hydrogen bonds are determined by an acceptor···donor distance of <3.5 Å and acceptor···H-donor angle of >120°.

[b] Occupancy (%) is defined as the percentage of simulation time that a specific hydrogen bond exists